Simple PV Modeling Under Variable Operating Conditions

CHRISTOPHER JUN QIAN TEH[ID]1, **MICHEAL DRIEBERG**[ID]1, **(Member, IEEE),**
SOCHEATRA SOEUNG[ID]1, **(Member, IEEE), AND RIZWAN AHMAD**[ID]2, **(Member, IEEE)**

[1]Department of Electrical and Electronic Engineering, Universiti Teknologi PETRONAS, Seri Iskandar 32610, Malaysia
[2]School of Electrical Engineering and Computer Science, National University of Sciences and Technology (NUST), Islamabad 44000, Pakistan

Corresponding author: Christopher Jun Qian Teh (christopher_19000229@utp.edu.my)

ABSTRACT Photovoltaic (PV) panels are increasingly used to convert sunlight into electricity, as a source of sustainable energy. It can be used in a wide variety of applications ranging from the well-known power generation to the emerging energy harvesting in Internet of Things (IoT). Hence, an accurate model is required to evaluate and predict the performance of the PV panel. However, the non-linear characteristics of PV panels make the modeling of their electrical response a challenging task. In the literature, most of the previous PV models have been developed for large wattage PVs under high irradiance, or for small wattage PVs under lower irradiance. Those that can model both usually require more information, including the I-V curves data at different irradiances, which is not always provided by the manufacturers. Therefore, this paper presents a simple PV modeling that can be applied for different wattage panels at different operating levels of irradiance, using only the commonly provided datasheet values at standard test condition (STC). The model uses the characteristic points translation technique to translate the short circuit current, open circuit voltage and maximum power voltage points, at STC to other operating conditions. These translated values are then used by the parameter extraction technique to extract the model's parameters. The proposed model's techniques can model the losses across the resistors at low irradiance, which reduces the error. The accuracy of the proposed model is validated using two representative commercial PV panels. Results are generated for the proposed model and other comparative works. The results show that the proposed model can improve the accuracy over the other compared works, with a consistent percentage difference of below 5% across all levels of irradiances for both panels.

INDEX TERMS PV panels, characteristic point translation, five parameters, PV modeling.

I. INTRODUCTION

Photovoltaic (PV) panels are increasingly used to convert the abundant and freely available sunlight into electrical energy. Research and development over the years has yielded vast improvements in their efficiency and lowered their costs, leading to accelerating deployments. Today, PV panels are used in many applications. They range from the high-power industry of energy generation all the way to the low-power emerging energy harvesting for powering Internet of Things (IoT) devices. The former addresses the urgent issue of global warming, caused by the expanding consumption of traditional fossil fuels [1]. While the latter is a key enabling technology

for the successful deployment of IoT devices, whose numbers are expected to be in the billions.

A PV panel is constructed with wafer-based silicon cells and it can be connected either in series or parallel configurations to yield the desired voltage and current. There is a wide variety of PV panels, from high to low wattages for different applications. They also operate across different operating conditions from high to low irradiances. Furthermore, their non-linear characteristics make their accurate modeling even more challenging. Nevertheless, an accurate PV model is crucial in assessing the expected electrical response of various PV panels under any operating conditions, which include variations in the irradiance.

PV models use an equivalent circuit with a set of parameters that describe the behavior of PV panel. Among the PV

The associate editor coordinating the review of this manuscript and approving it for publication was Giovanni Pau[ID].

models that have been proposed in the literature [2]–[10], one diode model with two resistors is found to be the most popular model because the model offers great accuracy yet simple. One of the benefits of this model is that it incorporates the parallel resistor, which is used to describe the leakage current. This model contains a set of five parameters to describe the PV behavior.

Many studies have proposed methods such as optimization and analytical to find the model's parameters. In these works [11]–[19], optimization methods are used to extract the parameters. The drawback of optimization methods is that they require the I-V curve information to allow the algorithm to find the best fit. The optimization methods also require setting a range limit for different parameters, which may vary for different panels. Although this method offers high accuracy, it is traded off with the model applicability as not all panel manufacturers provide I-V curve information.

To overcome some of the shortcomings, analytical methods [20]–[28] are used to extract the parameters directly and with most of them requiring only datasheet values as input. The most common values that can be found in the datasheets are the values of the three characteristic points, which are short circuit current, open circuit voltage, and maximum power points. These values are obtained at standard test condition (STC), which refers to, average solar spectrum at an air mass of 1.5, 1000 W/m^2 irradiance, and cell temperature of 25°C. The analytical method can be applied to almost all PV panels because it only requires the datasheet values at STC, which is always provided by the manufacturer. However, their consistent accuracy across different panel wattages and irradiances can still be improved.

The analytical method in [20] has proposed a simple yet accurate parameter extraction technique for one diode model. The work uses the PV panel's maximum power point to derive the model's parameter. As a result, the model's accuracy is improved when compared to existing techniques. This work not only allows the modeling of PV panel at STC but also at other operating conditions. To achieve that, parameter scaling technique is implemented to scale the model's parameters to different operating conditions. However, the accuracy of the parameter scaling technique to degrade at low irradiance levels.

Not only that, the work in [21] has made a comparison of existing parameter scaling techniques and evaluate their performances at different irradiance levels. The results show that most of the techniques have good accuracy at STC condition. But the model's accuracy varies significantly at low irradiance levels although most techniques use a similar scaling approach. The work suggests that the parameter scaling technique should not be the primary technique to model the PV panel's behavior at different irradiance levels. In [22], the work also uses parameter scaling technique to scale the parameters. An adjustable series resistor is used to increase the model's accuracy by fitting the maximum power point as close as possible to the datasheet value. Yet, the model's percentage difference at low irradiance levels is more than 5%

compared to the datasheet values. Therefore, the technique proposed in these works are not suitable for low irradiance PV modeling due to the model's lack of accuracy.

As the parameter scaling technique does not meet the expected accuracy at low irradiance levels, another analytical work in [23] uses the values of characteristic points at specific operating conditions to extract the model's parameters. Despite that, those values are obtained through experiments as the datasheet gives values only at STC. Thus, this work is unable to model the behavior of the PV panels at different irradiance levels without conducting experiments.

Alternatively, the characteristic points can be obtained through the translation technique. This technique can translate the datasheet three characteristic points to the specific operating conditions without requiring experimental values. The work in [24] has proposed a translation technique that can achieve high accuracy at high irradiance levels, but it degrades as the irradiance levels decrease. This is due to the proposed voltage correction coefficient not able to provide an accurate translation for the open circuit voltage and maximum power voltage.

For the translation work in [25], [26], a new coefficient named irradiance factor is proposed to improve the technique's accuracy. The irradiance factor can predicts the relationship between irradiance levels and open circuit voltage accurately. But there is still lack of accuracy on the maximum power voltage at low irradiance levels. The error is more than 5% when compared to the datasheet. An improvement on the maximum power voltage translation has been made in the following work [27]. The work can translate the maximum power voltage accurately by using the initial series resistor to define the relationship between irradiance levels and maximum power voltage. However, the open circuit voltage translation proposed in this work is not accurate.

The parameters extraction and characteristic points translation techniques are very important for creating an accurate PV model. As discussed previously, the work in [20] offers a simple yet accurate parameter extraction technique compared to other works, but the accuracy degrades at low irradiance. Hence, the translation techniques in [25]–[27] are required to increase the accuracy of three characteristic points at low irradiance levels. With the combination of these techniques, the model can model the behavior of PV panel at all irradiance levels. Moreover, the proposed model can also model high and low wattage panels at different operating irradiance levels using only datasheet values at STC.

Following is the organization of the paper. One diode model with two resistors is presented in detail in Section II. Section III provides the one diode model parameter extraction technique at STC. Section IV discusses about the parameter scaling technique while Section V introduces the characteristic points translation technique. In Section VI, the results of different translation techniques are presented while Section VII concludes the paper.
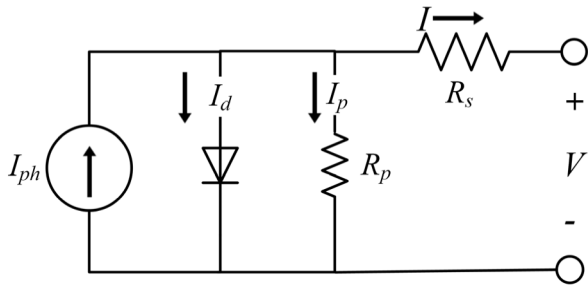
FIGURE 1. One diode model with two resistors.

II. ONE DIODE MODEL WITH TWO RESISTORS

The equivalent circuit of one diode model with two resistors is shown in Fig. 1. The circuit consists of photocurrent source, I_{ph}, the series resistor, R_s, the parallel resistor, R_p, and a diode. With reference to Fig. 1, the output current, I can be expressed as below by applying Kirchhoff's current law:

$$I = I_{ph} - I_d - \frac{V + IR_s}{R_p} \tag{1}$$

where I_d is the diode current and V is the voltage. The diode current can be further expressed by the Shockley diode equation which is described as follow:

$$I_d = I_o \left[\exp \left(\frac{q(V + IR_s)}{N_s akT} \right) - 1 \right] \tag{2}$$

By substituting (2) into (1), the model's output current equation is described as:

$$I = I_{ph} - I_o \left[\exp \left(\frac{q(V + IR_s)}{N_s akT} \right) - 1 \right] - \frac{V + IR_s}{R_p} \tag{3}$$

where I_o is the diode's saturation current, q is the electron charge, N_s is the number of series-connected of PV cells, a is the diode's ideality factor, k is the Boltzmann constant and T is the temperature.

III. PARAMETER EXTRACTION TECHNIQUE AT STC

The model consists of five parameters I_{ph}, I_o, a, R_s, and R_p which can be obtained through the parameter extraction technique proposed in work [20]. Firstly, the model's output current using (3) is evaluated at different operating conditions such as open circuit, short circuit, and maximum power.

At open circuit condition, $V = V_{oc}$ and $I = 0$. Therefore,

$$0 = I_{ph} - I_o \left[\exp \left(\frac{qV_{oc}}{N_s akT} \right) - 1 \right] - \frac{V_{oc}}{R_p} \tag{4}$$

At short circuit condition, $V = 0$ and $I = I_{sc}$. Therefore,

$$I_{sc} = I_{ph} - I_o \left[\exp \left(\frac{qR_s I_{sc}}{N_s akT} \right) - 1 \right] - \frac{R_s I_{sc}}{R_p} \tag{5}$$

At maximum power condition, $V = V_m$ and $I = I_m$. Therefore,

$$I_m = I_{ph} - I_o \left[\exp \left(\frac{q(V_m + I_m R_s)}{N_s akT} \right) - 1 \right] - \frac{V_m + I_m R_s}{R_p} \tag{6}$$

where I_{sc} is the short circuit current, I_m is the maximum power current, V_{oc} is the open circuit voltage and V_m is the maximum power voltage. By rearranging (4), the I_{ph} is given by:

$$I_{ph} = I_o \left[\exp \left(\frac{qV_{oc}}{N_s akT} \right) - 1 \right] + \frac{V_{oc}}{R_p} \tag{7}$$

By substituting (7) into (5), the I_o is written as:

$$I_{sc} = I_o \left[\exp \left(\frac{qV_{oc}}{N_s akT} \right) - 1 \right]$$
$$+ \frac{V_{oc}}{R_p} - I_o \left[\exp \left(\frac{qR_s I_{sc}}{N_s akT} \right) - 1 \right] - \frac{R_s I_{sc}}{R_p} \tag{8}$$

Simplifying the above equation:

$$I_{sc} = I_o \left[\exp \left(\frac{qV_{oc}}{N_s akT} \right) - \exp \left(\frac{qR_s I_{sc}}{N_s akT} \right) \right] + \frac{V_{oc} - R_s I_{sc}}{R_p} \tag{9}$$

The term $\exp(qR_s I_{sc}/N_s akT)$ can be neglected due to its insignificant value compared to $\exp(qV_{oc}/N_s akT)$. By rearranging (9), I_o is written as:

$$I_o = \left(I_{sc} - \frac{V_{oc} - I_{sc} R_s}{R_p} \right) \exp \left(-\frac{qV_{oc}}{aN_s kT} \right) \tag{10}$$

In order to get a more accurate expression for the parameter R_s and R_p, the work [20] proposed to include the number of parallel-connected PV cells, N_p in (3). Hence the new equation for the model's output current is:

$$\frac{I}{N_p} = I_{ph} - I_o \left[\exp \left(\frac{q(VN_p + IR_s N_s)}{N_p N_s akT} \right) - 1 \right]$$
$$- \frac{VN_p + IR_s N_s}{N_p N_s R_p} \tag{11}$$

To derive R_s, the term $(VN_p + IR_s N_s)/(N_p N_s R_p)$ can be neglected as the current flow across the parallel resistor is small. Then, the equation is evaluated at short circuit condition:

$$\frac{I_{sc}}{N_p} = I_{ph} - I_o \left[\exp \left(\frac{q(I_{sc} R_s)}{N_p akT} \right) - 1 \right] \tag{12}$$

and open circuit condition:

$$0 = I_{ph} - I_o \left[\exp \left(\frac{q(V_{oc})}{N_s akT} \right) - 1 \right] \tag{13}$$

By rearranging (12) and (13), a new expression of I_{ph} and I_o are derived and substituted into (11). The equation is written in (14).

$$I = \frac{I_{sc} \left[\exp \left(\frac{qV_{oc}}{N_s akT} \right) - 1 \right]}{\left[\exp \left(\frac{qV_{oc}}{N_s akT} \right) - \exp \left(\frac{qI_{sc} R_s}{N_p akT} \right) \right]}$$
$$- \frac{I_{sc} \left[\exp \left(\frac{q(VN_p + IR_s N_s)}{N_p N_s akT} \right) - 1 \right]}{\exp \left(\frac{qV_{oc}}{N_s akT} \right) - \exp \left(\frac{qI_{sc} R_s}{N_p akT} \right)} \tag{14}$$

To simplify (14), the term $\exp(qI_{sc} R_s/N_p akT)$ is assumed equal to one. This is because the value of a and T does not

significantly affect the overall term. Therefore, the simplified model's output current is shown:

$$I \simeq I_{sc} - \frac{I_{sc}\left[\exp\left(\frac{q(VN_p + IR_sN_s)}{N_pN_sakT}\right) - 1\right]}{\exp\left(\frac{qV_{oc}}{N_sakT}\right) - 1} \quad (15)$$

Evaluating (15) on the maximum power condition, the expression of R_s can be deduced as:

$$R_s = \frac{akTN_p}{qI_m}\ln\left[\exp\left(\frac{qV_{oc}}{akTN_s}\right) - \frac{I_m}{I_{sc}}\left\{\exp\left(\frac{qV_{oc}}{akTN_s}\right)\right\}\right] - \frac{V_mN_p}{I_mN_s} \quad (16)$$

On the other hand, the expression for R_p can be derived from the derivative of current with respect to voltage at maximum power point:

$$\left(\frac{dI}{dV}\right)\Big|_{MPP} = -\frac{I_m}{V_m} \quad (17)$$

To obtain the model's output current expression, (11) is evaluated at short circuit conditions:

$$\frac{I_{sc}}{N_p} = I_{ph} - I_o\left[\exp\left(\frac{q(I_{sc}R_s)}{N_pakT}\right) - 1\right] - \frac{I_{sc}R_s}{N_pR_p} \quad (18)$$

and open circuit conditions:

$$0 = I_{ph} - I_o\left[\exp\left(\frac{qV_{oc}}{N_sakT}\right) - 1\right] - \frac{V_{oc}}{N_sR_p} \quad (19)$$

By rearranging (18) and (19), a new expression of I_{ph} and I_o are derived and substituted into (11). The equation is written in (20). Substituting the derivative of (20), as shown at the bottom of the page, into (17), the expression of R_p is shown in (21), at the bottom of the page. For the value of parameter a, the work [20] proposed to increase its value from 0 until R_p reaches its minimum positive value. After the five parameters' values have been found, the R_s value can be increased to fit the maximum power point as close as possible, to the desired accuracy. Hence, the model's accuracy can be increased by using this technique

IV. PARAMETER SCALING TECHNIQUE
However, the parameters extracted at STC cannot be used to perform PV modeling at other operating conditions. This is because factors such as irradiance and temperature can affect the parameters and change the model's behavior. In the works [12] and [29]–[32], parameter scaling technique is used

to scale the model parameters from STC to other operating conditions. The five equations are shown below:

$$I_{ph} = \frac{G}{G_{STC}}[I_{sc,STC} + \alpha_{Isc}(T - T_{STC})] \quad (22)$$

$$I_o = I_{o,STC}\left(\frac{T}{T_{STC}}\right)^3\exp\left(\frac{1}{k}\left[\frac{E_{g,STC}}{T_{STC}} - \frac{E_g}{T}\right]\right) \quad (23)$$

$$a = a_{STC}\left(\frac{T}{T_{STC}}\right) \quad (24)$$

$$R_s = R_{s,STC}\left(\frac{T}{T_{STC}}\right)\left[1 - \beta_{Voc}\ln\frac{G}{G_{STC}}\right] \quad (25)$$

$$R_p = R_{p,STC}\frac{G_{STC}}{G} \quad (26)$$

where G_{STC}, $I_{sc,STC}$, T_{STC}, $I_{o,STC}$, a_{STC}, $R_{s,STC}$ and $R_{p,STC}$ are irradiance, short circuit current, temperature, diode saturation current, diode's ideality factor, series resistor and parallel resistor extracted at standard test condition. While G, T, I_{ph}, I_o, a, R_s and R_p are irradiance, short circuit current, temperature, diode saturation current, diode's ideality factor, series resistor and parallel resistor scaled at the specific operating condition. α_{Isc} is the current temperature coefficient and β_{Voc} is the voltage temperature coefficient of the PV panel. $E_{g,STC}$ is the material band gap energy where it is equal to 1.121eV for silicon cells.

According to [33], the photocurrent, I_{ph} changes linearly with solar irradiance, and it is also affected by the operating temperature. However, the work in [34] has suggested improvising the irradiance, G to effective irradiance instead, as there are reflectance losses that may occur on the PV panel's surface. The diode's saturation current I_o changes its values based on the diode theory, and a parameter is described as being proportional to the cell temperature based on the experiment [29]. Not only that, the series resistor R_s, plays a critical role in PV modeling as it determines the slope of I-V curve near the maximum power point. Therefore, the work in [29] and [35] proposed to decrease the value of R_s as the irradiance decreases. Nevertheless, the accuracy of R_s given by this equation at much lower irradiances can still be improved.

On the other hand, the parallel resistor's R_p value will affect the slope of the I-V curve near the short circuit current. An experiment has been conducted by the NIST (National Institute of Standard and Technology) to investigate the slope. Results show that the value of R_p increases when the

$$I = \frac{N_sI_{sc}(R_p + R_s) - N_pV + N_sIR_s}{N_sR_p} - \frac{(N_sI_{sc}(R_p + R_s) - N_pV_{oc})\left(\exp\left\{\frac{q(N_pV + N_sIR_s)}{akTN_sN_p}\right\} - 1\right)}{N_sR_p\left(\exp\left\{\frac{qV_{oc}}{akTN_s}\right\} - 1\right)} \quad (20)$$

$$R_p = \frac{[[N_sI_{sc}R_s - N_pV_{oc}][\exp(\frac{q(N_pV_m + N_sI_mR_s)}{(akTN_sN_p)})]q + akTN_sN_p[\exp\frac{(qV_{oc})}{(akTN_s)} - 1]]}{\frac{([N^2I_makTN_p(\exp(\frac{(qV_{oc})}{(akTN_s)}) - 1)]}{(V_mN_p - N_sI_mR_s)} - [\exp(\frac{q(N_pV_m + N_sI_mR_s)}{akTN_sN_p})]qN_sI_{sc}} \quad (21)$$

irradiance decreases. It is also can be expressed as inversely proportional to the irradiance level.

To validate this technique, an experiment [21] has been conducted and tested with commercially available PV panels. Results show that most I-V curves can achieve good accuracy at high irradiance levels, where the three characteristic points are very close to the experiment value. However, the accuracy starts to decrease when the parameters are scaled to lower irradiance.

V. CHARACTERISTIC POINTS TRANSLATION TECHNIQUE

As discussed in the previous section, there is lack of accuracy in parameter scaling technique at low irradiance levels. Thus, there is a need of an alternative technique to model the behavior at different operating conditions. Translation technique is chosen in this work as it requires only datasheet values to obtain the characteristic points values at different operating conditions. Below are the four equations proposed:

$$I_{sc} = I_{sc,STC}\left(\frac{G}{G_{STC}}\right)[1 + \alpha_{Isc}(T - T_{STC})] \tag{27}$$

$$I_{mp} = I_{mp,STC}\left(\frac{G}{G_{STC}}\right)[1 + \alpha_{Isc}(T - T_{STC})] \tag{28}$$

$$V_{oc} = \delta V_{oc,STC}\frac{T}{T_{STC}}\ln\left(\frac{G}{G_{STC}}\right) \\ + V_{oc,STC}\left(1 + \beta_{Voc}\left(T - T_{STC}\right)\right) \tag{29}$$

$$V_{mp} = V_{mp,STC} + [\delta V_{oc,STC}\frac{T}{T_{STC}}\ln\left(\frac{G}{G_{STC}}\right) \\ + V_{oc,STC}\left(1 + \beta_{Voc}\left(T - T_{STC}\right)\right) - V_{oc,STC}] \\ + R_{s0}\left(I_{mp,STC} - I_{mp,STC}\frac{G}{G_{STC}}[1 + \alpha_{Isc}(T - T_{STC})]\right) \tag{30}$$

Many of the existing works [36]–[40] show that the short circuit current and maximum power current of the PV panel changes proportionally to the irradiance and temperature. Moreover, the proposed translation of open circuit voltage also can be seen in the works [25], [26]. The translation uses the irradiance factor, δ to increase the translation's accuracy and it can be derived by using datasheet values shown in (31).

$$\delta = \frac{a}{V_{oc}} = \frac{1 - \beta_{Voc}T_{STC}}{50.1 - \alpha_{Isc}T_{STC}} \tag{31}$$

On the other hand, the translation of maximum power voltage also can be found in the work [27]. Initial series resistor, R_{s0} is used to model the losses across the series resistor which helps to increase the translation's accuracy. The initial series resistor is shown in (32), and it can be found using datasheet values too. By using these four proposed translation equations, the three characteristic points can be translated to other operating conditions by using only datasheet values.

$$R_{s0} = \frac{V_{mp} + \frac{(I_{mp}(V_{oc} - V_{mp}))}{(I_{sc} - I_{mp})\left(\ln\left(1 - \frac{I_{mp}}{I_{sc}}\right)\right)}}{I_{mp} + \frac{I_{mp}^2}{(I_{sc} - I_{mp})\left(\ln\left(1 - \frac{I_{mp}}{I_{sc}}\right)\right)}} \tag{32}$$

Next, some of the works have different translation equations for the open circuit voltage and maximum power voltage. This is because the voltage did not have the same response as the current. The works in [24] and [27] have proposed an equation for the open circuit voltage. The output current equation of the one diode model is evaluated at the open circuit condition and rearranged in (33). By substituting the parameter scaling from (22) and the I_o equation in (34) into (33), the translation of the open circuit voltage is shown in (35).

$$V_{oc} = \frac{N_s akT}{q}\ln\left(1 + \frac{I_{ph}}{I_o}\right) \tag{33}$$

$$I_o = \frac{I_{ph} + \alpha_{Isc}(T - T_{STC})}{\exp\left(\frac{q(V_{oc} + \beta_{Voc}(T - T_{STC}))}{N_s akT}\right) - 1} \tag{34}$$

$$V_{oc} = V_{oc,STC}(1 + \beta_{Voc}(T - T_{STC})) + V_{th}\ln\left(\frac{G}{G_{STC}}\right) \tag{35}$$

where $V_{th} = (aN_skT/q)$, is the thermal voltage of the PV panel. As there is an unknown diode ideality factor, a parameter in the thermal voltage, the work [41] proposed to use the nominal operating cell temperature (NOCT) that is provided in the datasheet to derive the parameter value. The expression of a is given as follows:

$$a = \frac{q(V_{oc,NOCT} - V_{oc,STC} - \beta_{Voc}(T - T_{STC}))}{N_s kT \ln\left(\frac{G}{G_{STC}}\right)} \tag{36}$$

The translation requires the open circuit voltage at NOCT, which is at 800 W/m² irradiance and the ambient temperature of 20 °C. However, most manufacturers did not provide the values at NOCT as it is seldom used. Therefore, the work in [28] proposed to set the value of a equal to 1, for simplicity.

Another work, [26] also proposed a translation technique for the open circuit voltage. The new equation for I_{ph} is shown in (37).

$$I_{ph} = I_o\left(\exp\left(\frac{V_{oc}}{a}\right)\right) \tag{37}$$

In order to obtain the translation for open circuit voltage, the parameter scaling from (22), (23) and (24) are required. By substituting them into (37), the translation is described as:

$$V_{oc} = a\frac{T}{T_{STC}}\ln\left(\frac{G}{G_{STC}}\right) + a\left(\frac{T}{T_{STC}}\right) \\ \times \ln\left[\frac{I_{ph}(1 + \alpha_{Isc}(T - T_{STC}))}{I_o\left(\frac{T}{T_{STC}}\right)^3 e^{47.1\left(1 - \frac{T_{STC}}{T}\right)}}\right] \tag{38}$$

To simplify (38), the second term can be approximately represented as the temperature dependency of the open circuit voltage as shown in (29). Compared to the works in [27], [28] and [42], irradiance factor, δ in (29) is proposed to improve the accuracy of the open circuit voltage. The a parameter is replaced by δ coefficient as it only requires datasheet values such as current and voltage temperature coefficient. To obtain the δ coefficient, the work uses (37) to evaluate

operating conditions at 1000 W/m^2 irradiance and arbitrary temperature. By using the parameter scaling from (22), (23), (24) and (35) into (37) and defined as:

$$
\begin{aligned}
(1 &+ \alpha_{Isc}(T - T_{STC}))I_{ph} \\
&= I_{o,STC} \left(\frac{T}{T_{STC}}\right)^3 \exp\left(\frac{1}{k}\left[\frac{E_{g,STC}}{T_{STC}} - \frac{E_g}{T}\right]\right) \\
&\times \exp\left(\frac{(1 + \beta_{Voc}(T - T_{STC}))\,V_{oc}}{a\frac{T}{T_{STC}}}\right)
\end{aligned}
\tag{39}
$$

To simplify (39), some modifications are applied to the equation, using (40) and (41):

$$
\frac{T}{T_{STC}} = \frac{T - T_{STC}}{T_{STC}} + 1
\tag{40}
$$

$$
\frac{1}{k}\left[\frac{E_{g,STC}}{T_{STC}} - \frac{E_g}{T}\right] = 47.1\left(\frac{\Delta T_c}{\Delta T_c + T_{STC}}\right)
\tag{41}
$$

where (41) is obtained using the equation of energy band gap of silicon, $E_g = E_{g,STC}(1\text{-}0.0002677(T\text{-}T_{STC}))$, the constant values $E_{g,STC} = 1.7958 \times 10^{-19}$ J, $k = 1.381 \times 10^{-23}$ J/K and $\Delta T_c = T\text{-}T_{STC}$. After substituting (40) and (41) into (39), a new equation in terms V_{oc} is shown below:

$$
\frac{a}{V_{oc}} = \frac{[1 - \beta_{Voc}T_{STC}]}{[f(\Delta T) + 47.1]}
\tag{42}
$$

$$
f(\Delta T) = \left(\frac{T_{STC}}{T - T_{STC}} + 1\right)\ln\left[\frac{\left(\frac{T-T_{STC}}{T_{STC}} + 1\right)^3}{1 + \alpha_{Isc}(T - T_{STC})}\right]
\tag{43}
$$

The term $f(\Delta T)$ varies in a limited range under arbitrary temperature for multiple PV panels as presented in [26]. Since the term $f(\Delta T)$ is not defined in $(T - T_{stc} = 0)$, therefore the corresponding limit is evaluated as follows:

$$
\begin{aligned}
\lim_{\Delta T \to 0} f(\Delta T) &= \lim_{\Delta T \to 0}\left(\frac{T_{STC}}{T - T_{STC}} + 1\right) \\
&\times \ln\left[\frac{\left(\frac{T-T_{STC}}{T_{STC}} + 1\right)^3}{1 + \alpha_{Isc}(T - T_{STC})}\right]
\end{aligned}
\tag{44}
$$

By solving (44), two equations, as shown in (45) and (46), and are substituted into (42) to form (31).

$$
3\ln\left[\lim_{\Delta T_c \to 0}\left(\frac{T - T_{STC}}{T_{STC}} + 1\right)^{\frac{T_{STC}}{T-T_{STC}}}\right] = 3\ln(e^1) = 3
\tag{45}
$$

$$
\ln\left[\lim_{\Delta T_c \to 0}(1 + \alpha_{Isc}(T - T_{STC}))^{\frac{T_{STC}}{T-T_{STC}}}\right] = \ln\left(e^{\alpha_{Isc}T_{STC}}\right)
$$
$$
= \alpha_{Isc}T_{STC}
\tag{46}
$$

For the maximum power voltage translation, the works in [24] and [42] proposed that it has the similar response as the open circuit voltage. However, this translation may not be implementable if the manufacturer did not provide the NOCT values, on which the V_{th} is derived from.

$$
V_{mp} = V_{mp,STC}(1 + \beta_{Voc}(T - T_{STC})) + V_{th}\ln\left(\frac{G}{G_{STC}}\right)
\tag{47}
$$

On the other hand, the work in [27] proposed an alternative translation for the maximum power voltage, as follows:

$$
V_{mp} = V_{mp,STC} + [V_{oc} - V_{oc,STC}] + R_{s0}(I_{mp,STC} - I_{mp})
\tag{48}
$$

By replacing the translated open circuit voltage in (48) with (29) and the translated maximum power current in (28), the equation for maximum power voltage is (30). However, the value of initial series resistor R_{s0} is unknown. The method proposed in [27] uses (3) to find its value. If an I-V curve has a slope that is almost zero at short circuit, then the value of parallel resistor R_p can be assumed as infinite. Hence, the last term in (3) can be ignored and by replacing I_{ph} with I_{sc}, the equation will become:

$$
I = I_{sc} - I_o\left(\exp\left(\frac{q(V + IR_s)}{N_s akT}\right) - 1\right)
\tag{49}
$$

When the PV model is in open circuit condition, (49) is solved as follows:

$$
\frac{\ln\left(\frac{I_{sc}}{I_o} + 1\right)}{V_{oc}} = \frac{q}{N_s akT}
\tag{50}
$$

By substituting (50) into (49), (51) is formed.

$$
I = I_{sc}\left[1 - \frac{I_o}{I_{sc}}\left(\exp\left(\frac{\ln\left(\frac{I_{sc}}{I_o} + 1\right)(V + IR_s)}{V_{oc}}\right) - 1\right)\right]
\tag{51}
$$

To simplify (51), a new coefficient is introduced where $z = I_{sc}/I_o$. Hence, the new current output equation is shown in (52).

$$
I = I_{sc}\left[1 - \left\{z^{\frac{(V+IR_s)}{V_{oc}} - 1}\right\}\right]
\tag{52}
$$

By evaluating (52) at maximum power conditions, the coefficient z can be solved as (53) and the derivative can be solved as (54).

$$
z = \left(1 - \frac{I_{mp}}{I_{sc}}\right)^{\frac{1}{\frac{V_{mp}+I_{mp}R_s}{V_{oc}} - 1}}
\tag{53}
$$

$$
-\frac{I_{mp}}{V_{mp}} = -I_{sc}\frac{1 + R_s\left(-\frac{I_{mp}}{V_{mp}}\right)}{V_{oc}}z^{\frac{V_{mp}+I_{mp}R_s}{V_{oc}} - 1}\ln z
\tag{54}
$$

To obtain the value of R_{s0}, (53) is substituted into (54) and the expression is (32).

Multiple types of voltage translation equations proposed from different works are discussed. The open circuit voltage [26] and maximum power voltage [27] give a direct translation using only datasheet values which is very convenient. Therefore, the equations from (27), (28), (29), (30), (31) and (32) are implemented in this work to translate the characteristic points from STC to other operating conditions.

After obtaining the translated characteristic points, these values will be used to extract the model's parameters and the procedures are shown in Fig. 2. Newton Raphson method is used to generate the model's I-V curve. The model's values
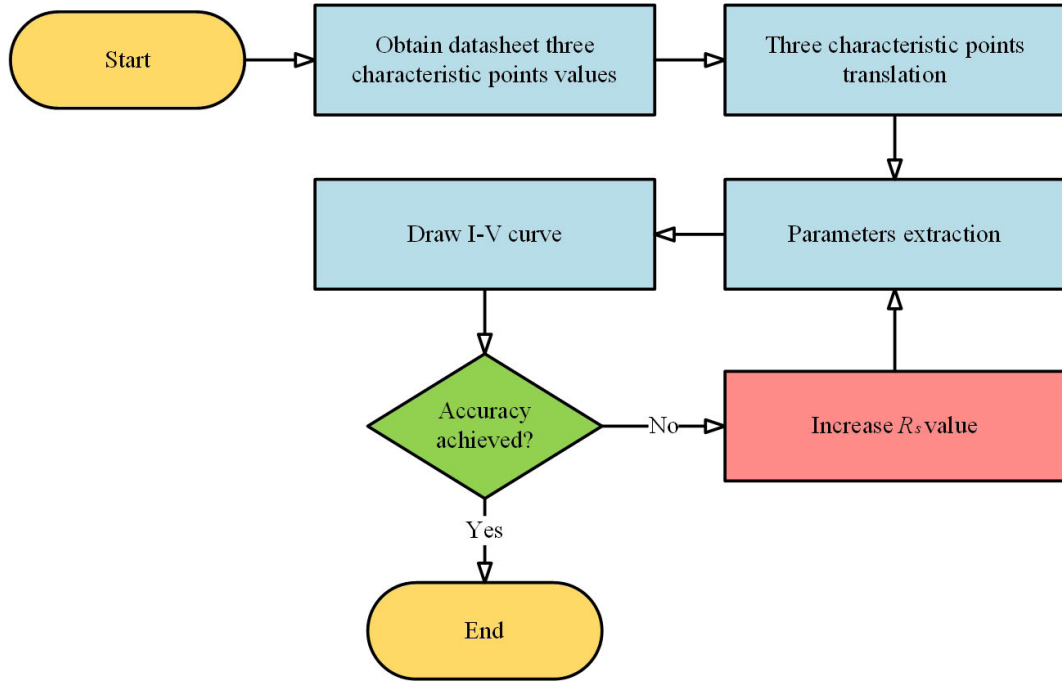
FIGURE 2. PV modeling flowchart.

I_m, V_m, I_{sc} and V_{oc} are obtained and compared with the datasheet values from 200 to 1000 W/m^2. If the values did not meet the accuracy, the value of parameter R_s will be increased to fit the maximum power point as close as possible.

Not only that, the proposed model also has a different and novel approach when compared to the other works in the literature. The latter implements the parameter extraction technique first to find the model's parameter at STC. This is followed by the parameter scaling/translation technique for other operating conditions. However, this results in decreased accuracy at low irradiance levels, due to the limitations of the latter technique. In contrast, the novelty of the proposed model comes from by implementing the best translation technique first to find the three characteristic points at different irradiance levels. Then, it is combined with the parameter extraction technique, which include the iteratively determined R_s value. At each iteration, the R_s value is increased during the parameter extraction technique process so that the corresponding I-V curve's maximum power point is as close as possible to the translated characteristic points. Hence, the order and combination of both the translation and parameter extraction techniques, are expected to improve the model's accuracy, especially at low irradiance levels.

VI. RESULTS AND DISCUSSION

Two commercial PV panels, KC200GT (200 Watts) and CNPV-5M (5 Watts) are used for the evaluation of the models. The KC200GT is chosen to represent the high power application in power generation [43], [44], while CNPV5M can represent the low power application such as IoT [45]–[48]. The values of three characteristic points between the model and datasheet are compared. The main reason for choosing

TABLE 1. Pv panels datasheet specifications.

Specifications at STC	PV Panels	
	CNPV–5M	KC200GT
$I_{mp,STC}$ (A)	0.2800	7.610
$V_{mp,STC}$ (V)	18.000	26.300
$V_{oc,STC}$ (V)	22.500	32.900
$I_{sc,STC}$ (A)	0.310	8.210
α_{Isc} (%/°C)	0.050	0.039
β_{Voc} (%/°C)	-0.300	-0.370
Number of cells	36.00	54.000

these PV panels is that the manufacturer has provided the I-V curves for 1000, 800, 600, 400 and 200 W/m^2 in the datasheet. However, these information were only provided at 25°C. Therefore, the results can only be compared at this temperature. To obtain the accurate values from the datasheet I-V curves, the GRABIT function from MATLAB is used. The specifications of both panels are summarized in Table 1.

Few works such as Al-Wahed and Abdullateef [24], Batzelis [26], and Ghandi *et al.* [27] are used for comparison with the proposed model. Both Wahed and Ghandi's works have implemented the parameter extraction technique and characteristic points translation similar to the proposed model. However, Batzelis did not implement the parameter extraction technique due to the complexity involved in the modeling process. Hence, Batzelis improvised the characteristic point translation technique to give a simple and straightforward voltage equation. In contrast, this improvisation
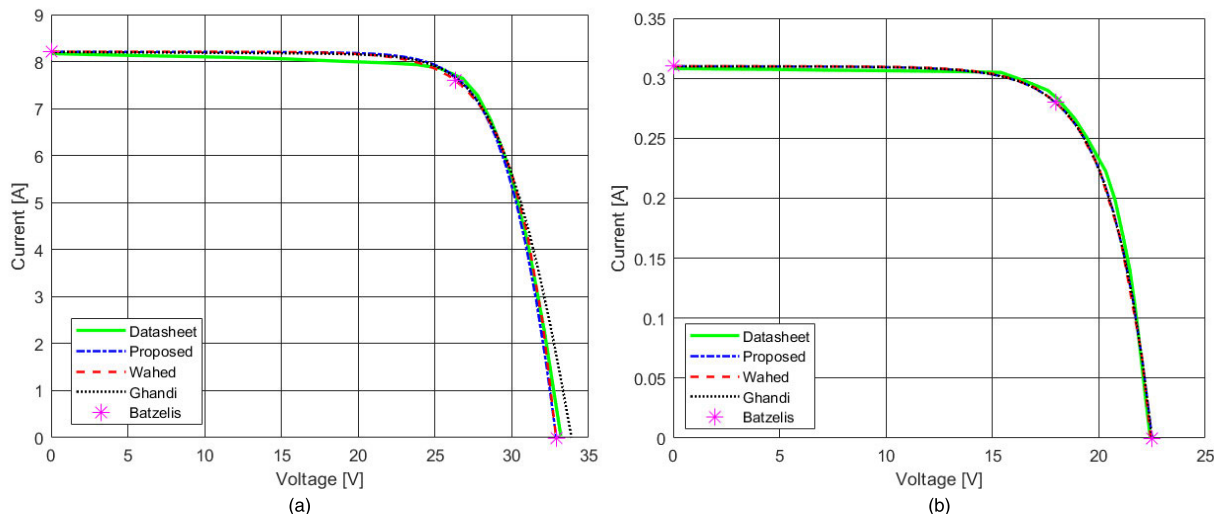
FIGURE 3. Comparison of I-V curve obtained from different methods with datasheet values at 1000 W/m^2. (a) KC200GT (b) CNPV-5M.
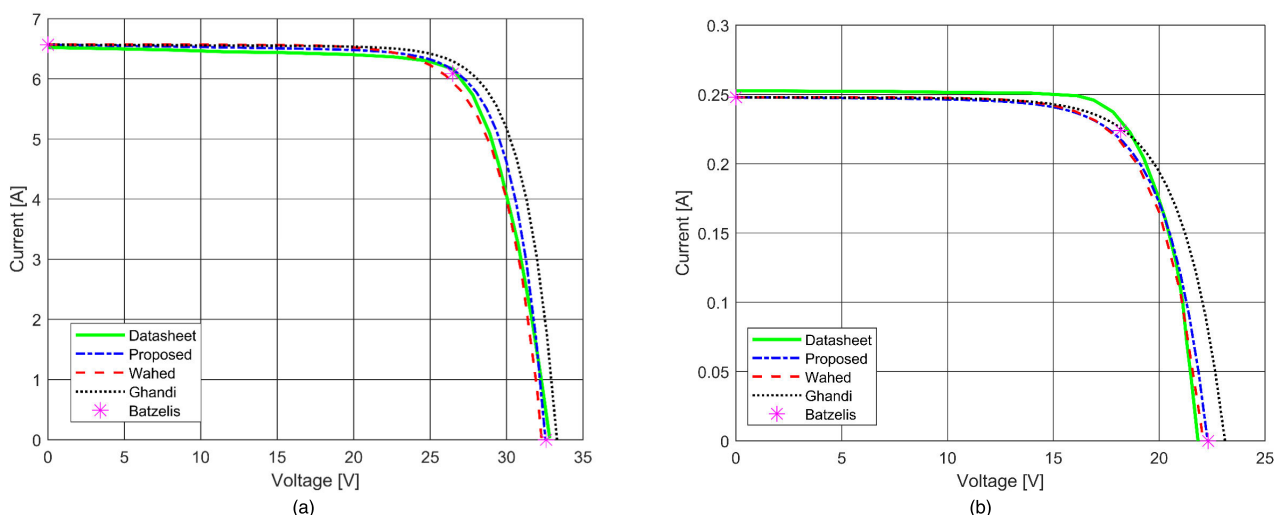
FIGURE 4. Comparison of I-V curve obtained from different methods with datasheet values at 800 W/m^2. (a) KC200GT (b) CNPV-5M.

drawback is that the technique can only provide the three characteristic points, rather than the entire I-V curve.

The results of the proposed model and discussed works are shown in Figs. 3-7. Fig. 3 shows the I-V curves generated from both panels at 1000 W/m^2 irradiance level. Most of the works fit very closely to the datasheet although Ghandi has a little overshoot at the open circuit voltage for 200 W panel. The overshoot is acceptable, as the percentage difference did not exceed 5% when compared to the datasheet values. However, as the irradiance level reduces, the accuracy of these works start to degrade. For example, at 800 W/m^2 for 5 W panel, Ghandi's technique has overshoot the open circuit voltage by more than 5%. The I-V curves of the other works also start to diverge after the maximum power point. Nevertheless, with Batzelis' improvised translation technique, the three characteristic points' values show a good fit with the datasheet.

At 600 W/m^2, the discussed works' I-V curves for both panels did not differ significantly as they are able to provide

results that are close to the datasheet values. While at 400 W/m^2, Wahed has generated an undershoot in the I-V curve for the 200 W panel where the maximum power point and open circuit voltage differ from the datasheet values. Nevertheless, the undershoot still falls below 5% difference. For the 5 W panel, Ghandi and the proposed model's I-V curves are very close to the datasheet I-V curve, from the short circuit point until the maximum power point. On the other hand, Wahed has a better match on the open circuit voltage while Batzelis' accuracy suffers at the maximum power voltage.

At 200 W/m^2, the I-V curves generated for both panels show that Wahed is not able to predict the PV behaviour accurately at low light conditions. Moreover, Batzelis also faced difficulties at low light conditions where the maximum power point is not accurate, especially for the 5 W panel. Similarly, Ghandi's I-V curve has exceeded the limit of 5%. It is important to note that the proposed model can accurately match the I-V curves at all irradiances for both panels.
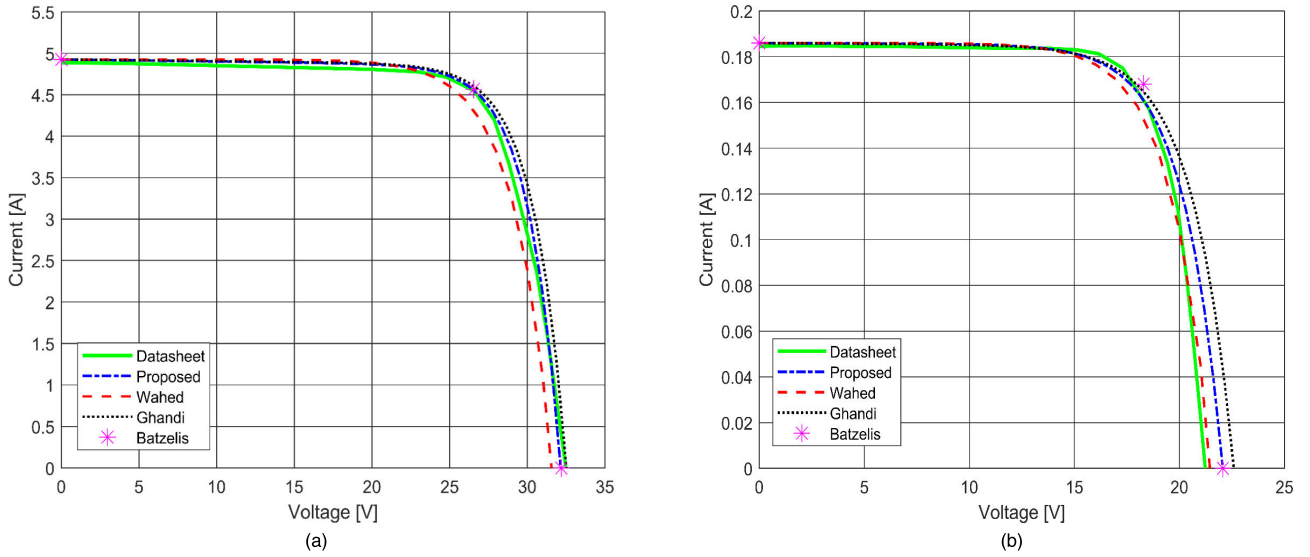
FIGURE 5. Comparison of I-V curve obtained from different methods with datasheet values at 600 W/m^2. (a) KC200GT (b) CNPV-5M.
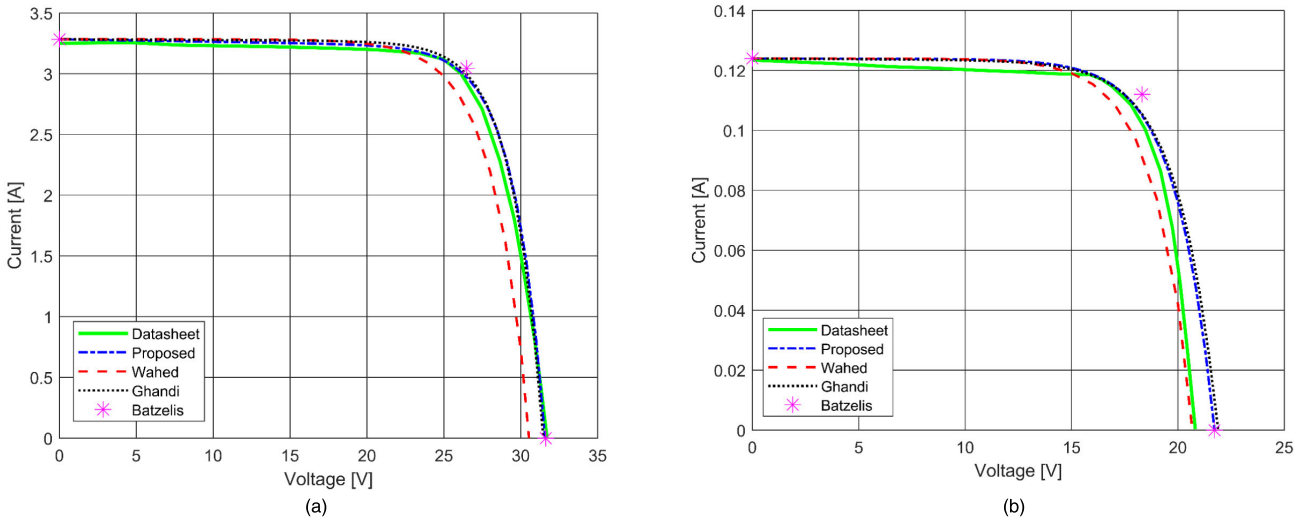
FIGURE 6. Comparison of I-V curve obtained from different methods with datasheet values at 400 W/m^2. (a) KC200GT (b) CNPV-5M.
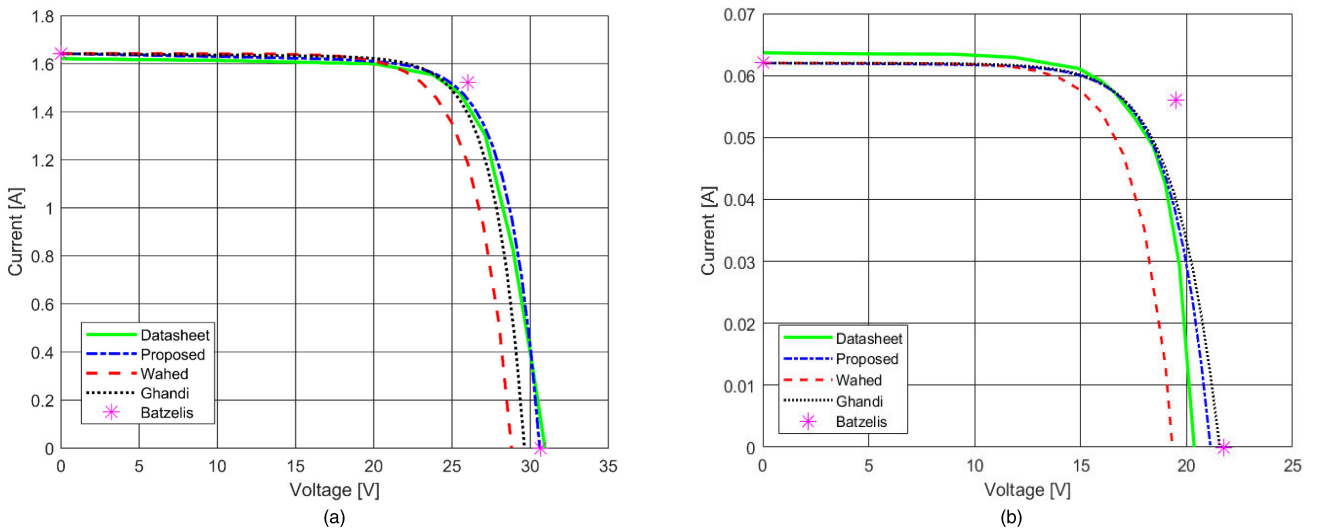
FIGURE 7. Comparison of I-V curve obtained from different methods with datasheet values at 200 W/m^2. (a) KC200GT (b) CNPV-5M.

TABLE 2. KC200GT Pv panels data comparison.

Irra-diance (W/m²)	Para-meters	Data					Percentage Difference between Datasheet and (%)			
		Datasheet	Proposed	Wahed	Batzelis	Ghandi	Proposed	Wahed	Batzelis	Ghandi
1000	I_{mp} (A)	7.610	7.679	7.418	7.610	7.542	0.907	2.523	0.000	0.894
	V_{mp} (V)	26.300	26.320	27.000	26.300	26.440	0.076	2.660	0.000	0.532
	V_{oc} (V)	32.900	32.800	32.810	32.900	33.522	0.300	0.274	0.000	1.884
	I_{sc} (A)	8.210	8.209	8.210	8.210	8.208	0.012	0.000	0.000	0.024
800	I_{mp} (A)	6.164	6.027	6.058	6.088	6.025	2.223	1.720	1.233	2.255
	V_{mp} (V)	26.499	27.370	26.000	26.467	26.982	3.287	1.883	0.121	1.823
	V_{oc} (V)	32.820	32.582	32.100	32.589	33.310	0.725	2.194	0.704	1.493
	I_{sc} (A)	6.522	6.568	6.568	6.568	6.568	0.705	0.705	0.705	0.705
600	I_{mp} (A)	4.547	4.455	4.439	4.566	4.477	2.023	2.375	0.418	1.539
	V_{mp} (V)	26.582	27.028	26.000	26.548	27.344	1.678	2.189	0.128	2.867
	V_{oc} (V)	32.475	32.100	31.550	32.189	32.400	1.155	2.848	0.881	0.231
	I_{sc} (A)	4.884	4.926	4.926	4.926	4.926	0.860	0.860	0.860	0.860
400	I_{mp} (A)	3.002	3.054	2.981	3.044	3.002	1.732	0.700	1.400	0.000
	V_{mp} (V)	26.113	25.913	25.000	26.472	26.466	0.766	4.262	1.375	1.275
	V_{oc} (V)	31.324	30.969	30.550	31.625	30.854	1.133	2.471	0.961	1.500
	I_{sc} (A)	3.251	3.284	3.284	3.284	3.284	1.015	1.015	1.015	1.015
200	I_{mp} (A)	1.475	1.510	1.525	1.522	1.498	2.373	3.390	3.186	1.559
	V_{mp} (V)	25.536	25.108	23.000	26.012	24.911	1.676	9.931	1.864	2.448
	V_{oc} (V)	30.107	30.007	28.800	30.660	29.600	0.332	4.341	1.837	1.684
	I_{sc} (A)	1.621	1.642	1.642	1.642	1.642	1.295	1.295	1.295	1.295

The value of three characteristics points of both panels obtained from datasheets and the discussed works are shown in Table 2 and Table 3. At 1000 W/m² irradiance level, the discussed works can achieve a low percentage difference for both panels. Only Wahed has a slightly higher percentage difference of 2.660% for the 200 W panel. However, higher percentage errors are generated for the 5 W panel as the irradiance level decreases. At 800 W/m², Table 3 shows that Wahed has generated a percentage difference of 5.603% on the maximum power current. It can also be noted that, Ghandi has generated a percentage difference of 7.444% on the open circuit voltage, which is more than 4 times when compared to the proposed model's 1.655%.

Starting from 600 W/m², Batzelis has difficulties in accurately modeling the maximum power voltage for the 5 W panel. For example, Batzelis has a percentage difference of 5.788% due to the irradiance factor of maximum power voltage used in the translation technique. The irradiance factor uses the Lambert function and parameter scaling technique to translate the maximum power voltage when the irradiance level changes. However, some ideal state of condition assumptions are made to simplify the process. Therefore, the irradiance factor is unable to model the losses across the resistor accurately at low irradiance levels.

At 400 W/m², Ghandi and Batzelis have generated inaccurate maximum power voltage and open circuit voltage for the 5 W panel. Ghandi used an iterative thermal voltage to translate the open circuit voltage. By applying it iteratively, it tries to fit the characteristic point as close as possible to the datasheet. Although its accuracy is acceptable for the 200 W panel at the same irradiance level, but the accuracy degrades for the 5 W panel, which is at 5.170%. This is because the iterative process is unable to provide an accurate fit for low wattage panels with a low number of PV cells. Moreover, it can be noted that Batzelis' accuracy for the maximum power voltage continues to suffer, with an even higher difference of 8.039%, due to the irradiance factor mentioned previously. In comparison, the proposed model provided a significant 3-fold improvement with 2.377%.

A similar situation also happened at 200 W/m², where most of the works are unable to translate the characteristic points accurately. The translation technique proposed by Batzelis has a 17.228% difference on maximum power voltage and 6.970% difference on the open circuit voltage for the 5 W panel. It can be generally observed that Batzelis' performance is inferior for the lower wattage panel. Ghandi is better but also has a 5.934% difference on the open circuit voltage for the 5 W panel. Although Wahed's iterative thermal voltage

TABLE 3. CNPV-5M Pv panels data comparison.

Irra-diance (W/m²)	Para-meters	Data					Percentage Difference between Datasheet and (%)			
		Datasheet	Proposed	Wahed	Batzelis	Ghandi	Proposed	Wahed	Batzelis	Ghandi
1000	I_{mp} (A)	0.280	0.279	0.280	0.280	0.279	0.357	0.000	0.000	0.000
	V_{mp} (V)	18.000	18.000	18.000	18.000	18.000	0.000	0.000	0.000	0.000
	V_{oc} (V)	22.500	22.500	22.500	22.500	22.500	0.000	0.000	0.000	0.000
	I_{sc} (A)	0.310	0.310	0.310	0.310	0.310	0.000	0.000	0.000	0.000
800	I_{mp} (A)	0.232	0.222	0.219	0.224	0.222	4.310	5.603	3.448	4.310
	V_{mp} (V)	17.819	17.847	18.000	18.173	18.486	0.157	1.015	1.986	3.743
	V_{oc} (V)	21.507	21.863	22.000	22.310	23.108	1.655	2.292	3.733	7.444
	I_{sc} (A)	0.253	0.248	0.248	0.248	0.248	1.976	1.976	1.976	1.976
600	I_{mp} (A)	0.175	0.168	0.170	0.167	0.167	4.000	2.857	4.000	4.571
	V_{mp} (V)	17.292	17.641	17.000	17.622	18.082	2.018	1.688	5.788	4.568
	V_{oc} (V)	21.232	22.051	21.000	21.587	22.150	3.857	1.092	3.918	4.323
	I_{sc} (A)	0.185	0.186	0.186	0.186	0.186	0.540	0.540	0.540	0.540
400	I_{mp} (A)	0.114	0.112	0.113	0.112	0.112	1.754	0.877	1.754	1.754
	V_{mp} (V)	16.953	17.356	16.173	18.316	17.511	2.377	4.600	8.039	3.2914
	V_{oc} (V)	20.813	21.695	20.734	21.718	21.889	4.237	0.379	4.348	5.17
	I_{sc} (A)	0.123	0.124	0.124	0.124	0.124	0.813	0.813	0.813	0.813
200	I_{mp} (A)	0.057	0.056	0.058	0.056	0.055	1.754	1.754	1.754	3.508
	V_{mp} (V)	16.635	16.447	15.000	19.501	17.251	1.130	9.828	17.228	3.703
	V_{oc} (V)	20.356	21.086	19.220	21.775	21.564	3.586	5.580	6.970	5.934
	I_{sc} (A)	0.064	0.062	0.062	0.062	0.062	3.125	3.125	3.125	3.125

can accurately translate most of the characteristic points at high irradiance levels, but the percentage difference at low irradiance for both panels is relatively high. The results show a 9.931% and 9.828% differences on the maximum power voltages, and 5.580% difference on the open circuit voltage. On the other hand, the proposed model results showed differences of only 1.676% and 1.130%, which is a significant improvement of several folds.

The results in Table 2 and 3 show that the proposed model can consistently achieve an overall lower percentage difference when compared to other works at different irradiance levels. The highest percentage difference generated is 4.237% on the open circuit voltage for the 5 W panel, which is still acceptable as it is still below 5%. The proposed model achieves this by combining the best features from Fahad's parameter extraction technique and selective translation techniques from Batzelis and Ghandi. The improved accuracy of the proposed model results over the compared works highlights its importance and contribution.

Based on the discussion of the other works' performance, it can be summarized that Batzelis has the highest percentage difference for the 5 W panel's maximum power voltage due to limitations of the irradiance factor. On the other

hand, Ghandi also struggles to provide an accurate open circuit voltage due to the iterative thermal voltage. Therefore, the improved accuracy of the proposed model is due to the use of translation techniques for open circuit voltage from Batzelis and maximum power voltage from Ghandi. Batzelis uses the datasheet's temperature coefficient to predict the behavior of open circuit voltage, which is better than Ghandi and Wahed's iterative thermal voltage. Furthermore, Ghandi also uses the initial series resistor to model the losses at different irradiance levels, which reduces the errors during the translation, especially for the maximum power voltage. All of these works use the same translation for short circuit current and maximum power current. Hence, the observed minimal differences among them.

VII. CONCLUSION

In this paper, one diode with two resistors PV model with improved characteristic points translation and parameter extraction techniques has been presented. The inputs in both characteristic point translation and parameter extraction techniques are based on datasheet values, which is analytical and simple. Then, the proposed model was compared with datasheet values and few similar works to verify its accuracy.

Results show that the proposed model can achieve a consistently higher accuracy, with a percentage difference of less than 5% at all irradiance levels for both PV panels. Although other works can achieve a lower percentage difference, but their accuracy lacks consistency for both panels at all irradiance levels. Therefore, it can be concluded that the proposed model can model the PV behavior at different irradiance levels for high and low wattage panels, at a consistently high level of accuracy. The investigation of the proposed model at different temperatures and with two diode model are interesting directions for future works.

REFERENCES

[1] R. Elgohary, A. A. A. Elela, and A. Elkholy, "Electrical characteristics modeling for photovoltaic modules based on single and two diode models," in *Proc. 12th Int. MEPCON Conf.*, Dec. 2018, pp. 685–688.

[2] H. M. El-Helw, A. Magdy, and M. I. Marei, "A hybrid maximum power point tracking technique for partially shaded photovoltaic arrays," *IEEE Access*, vol. 5, pp. 11900–11908, 2017.

[3] Z. Yan, C. Li, Z. Song, L. Xiong, and C. Luo, "An improved brain storming optimization algorithm for estimating parameters of photovoltaic models," *IEEE Access*, vol. 7, pp. 77629–77641, 2019.

[4] W. Li, G. Zhang, T. Pan, Z. Zhang, Y. Geng, and J. Wang, "A Lipschitz optimization-based MPPT algorithm for photovoltaic system under partial shading condition," *IEEE Access*, vol. 7, pp. 126323–126333, 2019.

[5] Q. Hao, Z. Zhou, Z. Wei, and G. Chen, "Parameters identification of photovoltaic models using a multi-strategy success-history-based adaptive differential evolution," *IEEE Access*, vol. 8, pp. 35979–35994, 2020.

[6] W. Zhang, G. Zhou, H. Ni, and Y. Sun, "A modified hybrid maximum power point tracking method for photovoltaic arrays under partially shading condition," *IEEE Access*, vol. 7, pp. 160091–160100, 2019.

[7] Z. Liao, Z. Chen, and S. Li, "Parameters extraction of photovoltaic models using triple-phase teaching-learning-based optimization," *IEEE Access*, vol. 8, pp. 69937–69952, 2020.

[8] D. Yousri, T. S. Babu, E. Beshr, M. B. Eteiba, and D. Allam, "A robust strategy based on marine predators algorithm for large scale photovoltaic array reconfiguration to mitigate the partial shading effect on the performance of PV system," *IEEE Access*, vol. 8, pp. 112407–112426, 2020.

[9] T. Huang, C. Zhang, H. Ouyang, G. Luo, S. Li, and D. Zou, "Parameter identification for photovoltaic models using an improved learning search algorithm," *IEEE Access*, vol. 8, pp. 116292–116309, 2020.

[10] A. A. Z. Diab, H. M. Sultan, R. Aljendy, A. S. Al-Sumaiti, M. Shoyama, and Z. M. Ali, "Tree growth based optimization algorithm for parameter extraction of different models of photovoltaic cells and modules," *IEEE Access*, vol. 8, pp. 119668–119687, 2020.

[11] Z. Amokrane, M. Haddadi, and N. O. Cherchali, "An improved technique based on PSO to estimate the parameters of the solar cell and photovoltaic module," in *Proc. ICAIRES*, 2018, pp. 439–449.

[12] S. P. Aly, S. Ahzi, and N. Barth, "An adaptive modelling technique for parameters extraction of photovoltaic devices under varying sunlight and temperature conditions," *Appl. Energy*, vol. 236, pp. 728–742, Feb. 2019.

[13] A. A. El-Fergany, "Parameters identification of PV model using improved slime mould optimizer and Lambert W-function," *Energy Rep.*, vol. 7, pp. 875–887, Nov. 2021.

[14] J. Wang, B. Yang, D. Li, C. Zeng, Y. Chen, Z. Guo, X. Zhang, T. Tan, H. Shu, and T. Yu, "Photovoltaic cell parameter estimation based on improved equilibrium optimizer algorithm," *Energy Convers. Manage.*, vol. 236, May 2021, Art. no. 114051.

[15] M.-U.-N. Khursheed, M. A. Alghamdi, M. F. N. Khan, A. K. Khan, I. Khan, A. Ahmed, A. T. Kiani, and M. A. Khan, "PV model parameter estimation using modified FPA with dynamic switch probability and step size function," *IEEE Access*, vol. 9, pp. 42027–42044, 2021.

[16] A. T. Kiani, M. F. Nadeem, A. Ahmed, I. Khan, R. M. Elavarasan, and N. Das, "Optimal PV parameter estimation via double exponential function-based dynamic inertia weight particle swarm optimization," *Energies*, vol. 13, no. 15, p. 4037, Aug. 2020.

[17] Y. Fan, P. Wang, A. A. Heidari, X. Zhao, H. Turabieh, and H. Chen, "Delayed dynamic step shuffling frog-leaping algorithm for optimal design of photovoltaic models," *Energy Rep.*, vol. 7, pp. 228–246, Nov. 2021.

[18] H. Rezk, T. S. Babu, M. Al-Dhaifallah, and H. A. Ziedan, "A robust parameter estimation approach based on stochastic fractal search optimization algorithm applied to solar PV parameters," *Energy Rep.*, vol. 7, pp. 620–640, Nov. 2021.

[19] W. Long, T. Wu, M. Xu, M. Tang, and S. Cai, "Parameters identification of photovoltaic models by using an enhanced adaptive butterfly optimization algorithm," *Energy*, vol. 229, Aug. 2021, Art. no. 120750.

[20] F. Rasool, M. Drieberg, N. Badruddin, and B. S. M. Singh, "PV panel modeling with improved parameter extraction technique," *Sol. Energy*, vol. 153, pp. 519–530, Sep. 2017.

[21] S. Bader, X. Ma, and B. Oelmann, "One-diode photovoltaic model parameters at indoor illumination levels—A comparison," *Sol. Energy*, vol. 180, pp. 707–716, Mar. 2019.

[22] R. A. P. Franco and F. H. T. Vieira, "Analytical method for extraction of the single-diode model parameters for photovoltaic panels from datasheet data," *Electron. Lett.*, vol. 54, no. 8, pp. 519–521, Apr. 2018.

[23] V. Lo Brano, A. Orioli, G. Ciulla, and A. Di Gangi, "An improved five-parameter model for photovoltaic modules," *Sol. Energy Mater. Sol. Cells*, vol. 94, no. 8, pp. 1358–1370, Aug. 2010.

[24] M. E. A. Al-Wahed and O. F. Abdullateef, "Modeling of monocrystalline PV cell considering ambient conditions in Baghdad city," *Al-Khwarizmi Eng. J.*, vol. 13, no. 3, pp. 74–82, Sep. 2017.

[25] E. I. Batzelis and S. A. Papathanassiou, "A method for the analytical extraction of the single-diode PV model parameters," *IEEE Trans. Sustain. Energy*, vol. 7, no. 2, pp. 504–512, Apr. 2016.

[26] E. I. Batzelis, "Simple PV performance equations theoretically well founded on the single-diode model," *IEEE J. Photovolt.*, vol. 7, no. 5, pp. 1400–1409, Sep. 2017.

[27] O. Gandhi, C. D. Rodriguez-Gallegos, N. B. Y. Gorla, M. Bieri, T. Reindl, and D. Srinivasan, "Reactive power cost from PV inverters considering inverter lifetime assessment," *IEEE Trans. Sustain. Energy*, vol. 10, no. 2, pp. 738–747, Apr. 2019.

[28] X. Ma, M. Li, L. Du, B. Qin, Y. Wang, X. Luo, and G. Li, "Online extraction of physical parameters of photovoltaic modules in a building-integrated photovoltaic system," *Energy Convers. Manage.*, vol. 199, Nov. 2019, Art. no. 112028.

[29] J. Bai, S. Liu, Y. Hao, Z. Zhang, M. Jiang, and Y. Zhang, "Development of a new compound method to extract the five parameters of PV modules," *Energy Convers. Manage.*, vol. 79, pp. 294–303, Mar. 2014.

[30] J. M. Raya-Armenta, P. R. Ortega, N. Bazmohammadi, S. V. Spataru, J. C. Vasquez, and J. M. Guerrero, "An accurate physical model for PV modules with improved approximations of series-shunt resistances," *IEEE J. Photovolt.*, vol. 11, no. 3, pp. 699–707, May 2021.

[31] C. S. Ruschel, F. P. Gasparin, and A. Krenzinger, "Experimental analysis of the single diode model parameters dependence on irradiance and temperature," *Sol. Energy*, vol. 217, pp. 134–144, Mar. 2021.

[32] A. Elkholy and A. A. A. El-Ela, "Optimal parameters estimation and modelling of photovoltaic modules using analytical method," *Heliyon*, vol. 5, no. 7, Jul. 2019, Art. no. e02137.

[33] Y. Chaibi, A. Allouhi, M. Malvoni, M. Salhi, and R. Saadani, "Solar irradiance and temperature influence on the photovoltaic cell equivalent-circuit models," *Sol. Energy*, vol. 188, pp. 1102–1110, Aug. 2019.

[34] M. Zaimi, H. El Achouby, A. Zegoudi, A. Ibral, and E. M. Assaid, "Numerical method and new analytical models for determining temporal changes of model-parameters to predict maximum power and efficiency of PV module operating outdoor under arbitrary conditions," *Energy Convers. Manage.*, vol. 220, Sep. 2020, Art. no. 113071.

[35] Y. Chaibi, A. Allouhi, and M. Salhi, "A simple iterative method to determine the electrical parameters of photovoltaic cell," *J. Cleaner Prod.*, vol. 269, Oct. 2020, Art. no. 122363.

[36] R. Khezzar, M. Zereg, and A. Khezzar, "Modeling improvement of the four parameter model for photovoltaic modules," *Sol. Energy*, vol. 110, pp. 452–462, Dec. 2014.

[37] R. Q. Nafil, H. T. Khamees, and M. S. Majeed, "Identification the internal parameters for mono-crystalline solar module using MATLAB-simulation and experimental ascertainment," *Telkomnika*, vol. 19, no. 3, p. 716, Jun. 2021.

[38] S. A. R. Zaidi, M. Ghogho, D. C. McLernon, and A. Swami, "Energy harvesting empowered cognitive metro-cellular networks," in *Proc. 1st Int. Workshop Cognit. Cellular Syst. (CCS)*, Sep. 2014, pp. 1–5.

[39] S. Jenkal, M. Ajaamoum, and A. Rachdy, "Modeling a photovoltaic emulator using four methods and buck-boost converter," *Engineering*, vol. 29, no. 2, pp. 1–8, 2021.

[40] S. Vergura, "A complete and simplified datasheet-based model of PV cells in variable environmental conditions for circuit simulation," *Energies*, vol. 9, no. 5, p. 326, Apr. 2016.

[41] H. El Achouby, M. Zaimi, A. Ibral, and E. M. Assaid, "New analytical approach for modelling effects of temperature and irradiance on physical parameters of photovoltaic solar module," *Energy Convers. Manage.*, vol. 177, pp. 258–271, Dec. 2018.

[42] W. Shinong, M. Qianlong, X. Jie, G. Yuan, and L. Shilin, "An improved mathematical model of photovoltaic cells based on datasheet information," *Sol. Energy*, vol. 199, pp. 437–446, Mar. 2020.

[43] M. H. Qais, H. M. Hasanien, S. Alghuwainem, and A. S. Nouh, "Coyote optimization algorithm for parameters extraction of three-diode photovoltaic models of photovoltaic modules," *Energy*, vol. 187, Nov. 2019, Art. no. 116001.

[44] B. S. S. G. Pardhu and V. R. Kota, "Radial movement optimization based parameter extraction of double diode model of solar photovoltaic cell," *Sol. Energy*, vol. 213, pp. 312–327, Jan. 2021.

[45] S. Zeadally, F. K. Shaikh, A. Talpur, and Q. Z. Sheng, "Design architectures for energy harvesting in the Internet of Things," *Renew. Sustain. Energy Rev.*, vol. 128, Aug. 2020, Art. no. 109901.

[46] J. Anzola, A. Jiménez, and G. Tarazona, "Self-sustainable power-collecting node in IoT," *Internet Things*, vol. 7, Sep. 2019, Art. no. 100082.

[47] O. Al-Shahri, F. Ismail, M. Hannan, M. Lipu, A. Al-Shetwi, R. Begum, N. Al-Muhsen, and E. Soujeri, "Solar photovoltaic energy optimization methods, challenges and issues: A comprehensive review," *J. Clean. Prod.*, vol. 284, pp. 1254–1272, Dec. 2021.

[48] A. Khattab, S. E. D. Habib, H. Ismail, S. Zayan, Y. Fahmy, and M. M. Khairy, "An IoT-based cognitive monitoring system for early plant disease forecast," *Comput. Electron. Agricult.*, vol. 166, Nov. 2019, Art. no. 105028.

MICHEAL DRIEBERG (Member, IEEE) received the B.Eng. degree in electrical and electronics engineering from Universiti Sains Malaysia, Penang, Malaysia, in 2001, the M.Sc. degree in electrical and electronics engineering from Universiti Teknologi PETRONAS, Seri Iskandar, Malaysia, in 2005, and the Ph.D. degree in electrical and electronics engineering from Victoria University, Melbourne, Australia, in 2011. He is currently a Senior Lecturer with the Department of Electrical and Electronics Engineering, Universiti Teknologi PETRONAS. He has made several contributions to the Wireless Broadband Standards Group. He has published and served as a reviewer for several high impact journals and flagship conferences. His research interests include radio resource management, medium access control protocols, energy harvesting communications, and performance analysis for wireless and sensor networks.

SOCHEATRA SOEUNG (Member, IEEE) was born in Phnom Penh, Cambodia, in 1986. He received the B.Eng. degree (Hons.) in electrical and electronic engineering, the M.Sc. degree (research) in PCB testing based on eddy current, and the Ph.D. degree (research) in RF microwave engineering from Universiti Teknologi PETRONAS, Malaysia, in 2010, 2013, and 2018, respectively. He worked as a Research Officer under project "Wireless Communication using Evaporation Duct (WiDuct)" with the responsibility to RF frontend design, implementation, and testing. He is currently a Lecturer with the Electrical and Electronic Engineering Department, Universiti Teknologi PETRONAS. His research interests include filter synthesis, design and implementation on planar and cavity microwave filters, and computer-aided tuning and optimization techniques. He is also a member of MTT and a Committee Member of the IEEE ED/MTT/SSC Penang Chapter, Malaysia.

RIZWAN AHMAD (Member, IEEE) received the M.Sc. degree in communication engineering and media technology from the University of Stuttgart, Stuttgart, Germany, in 2004, and the Ph.D. degree in electrical engineering from Victoria University, Melbourne, Australia, in 2010. From 2010 to 2012, he was a Postdoctoral Research Fellow with Qatar University, under the support of QNRF Grant. He is currently an Associate Professor with the School of Electrical Engineering and Computer Science, National University of Sciences and Technology, Pakistan. He has published and served as a reviewer for leading IEEE journals and conferences. His research interests include medium access control protocols, spectrum and energy efficiency, energy harvesting, and performance analysis for wireless communication and networks. He was a recipient of the prestigious International Postgraduate Research Scholarship from the Australian Government.

CHRISTOPHER JUN QIAN TEH received the degree (Hons.) in electrical and electronic engineering from Universiti Teknologi PETRONAS, in 2018, where he is currently pursuing the M.Sc. degree. He completed his internship as a Research Assistant in creating an acoustical sensor system to detect applied brakes of train wagons at the University of Applied Sciences Upper Austria.

● ● ●